Below we give our (now slightly modified) responses to referees, indicating where we have made modifications to the text in responses to referee comments. We believe we have addressed all the comments, although in one or two cases we have chosen not to make a change, believing the already published response was sufficient. We hope we have justified this in the text. We would like to thank all referees, as we believe all their comments have made for a better paper.

We did discover one numerical error in our previous published response to referees when we quoted a sensitivity improvement of 72 with respect to a measurement made at Q-band (now included in the SI). It is actually 24. This number and comparison was not mentioned in the original manuscript, and the correct number is included in the new manuscript but we would be keen to add a correction to our responses.

We then give a marked-up script showing where the paper has been changed. There are also a few very minor extra changes made in the uploaded document, not shown here, but these are all very minor typographical changes.

Graham and Hassane

Prof Graham Smith
Dr Hassane El Mkami

Reply to Comments from Gunnar Jeschke

The authors demonstrate convincingly that by using a high-power W-band spectrometer with an only weakly resonant shorted waveguide end instead of a microwave resonator, the problem of level-mixing related perturbation of large dipolar frequencies can be avoided. This problem makes extraction of distance distributions between Gd(III) labels precarious at distances shorter than 3 nm. Hence, the new approach solves an important problem for broader application of Gd(III)-Gd(III) distance measurements. Furthermore, the authors show convincingly that it can be advantageous to avoid excitation of the central transition of Gd(III) altogether in DEER experiments, which comes as a surprise. The manuscript is mostly clear and concise, the data is of high quality, and its analysis is mostly adequate. However, there are a few minor problems that require revision.

We would like to thank Prof Jeschke for his kind words and careful reading of the manuscript and his helpful comments and suggestions.

General:

1. **The text refers mostly to frequency offsets when discussing different excitation schemes, but the Figures use PnOn codes. Please give frequency offsets directly in figures.**

We are keen to keep the PnOn codes as they are used in all the tables and the text, and this scheme was chosen after examining a number of alternatives. However, we have now added frequency offsets to all the figures.

2. **The claim on similar data quality as with nitroxide labels would have been much more convincing at intermediate distances, where nitroxide labels can convincingly resolve an asymmetry of the distance distribution that is related to flexibility of the ruler backbone. For that, the 2.1 nm may be too short and the 6 nm slightly too long (at the maximum dipolar evolution time achieved here).**

This is a very good suggestion, and (co-author) Prof Godt also specifically suggested we check for this asymmetry. These is some evidence for asymmetry Gd-ruler (6.0 nm), but we do not see this at the shorter distance very possibly for the reasons the referee suggests. We have added a statement to that effect.

3. **section 65: Gd(III)-Gd(III) RIDME was first demonstrated and the overtone problem noticed in 2014 (DOI: 10.1021/jz502129t)**

This was an unfortunate oversight and we have added this reference.

4. **section 70: "applying the wormlike chain model". I do not find this in either the results section, discussion, or Supplementary Material.**

We agree the intended reference (Dalaloyan 2015) to this statement was not clear and we have now added a sentence to clarify.

5. **section 155: Why did you measure Tm, T1 only at the maximum of the Gd(III) spectrum? These relaxation times are known to differ between central and satellite transitions and you focus on satellite transitions. Please make at least a remark that differences are to be expected and cite literature for that.**

We completely agree measuring T_M and T_1 at the offset frequencies used would have been both helpful and highly appropriate. It was an initial oversight. Unfortunately, immediately following the set of experiments described in the paper, the spectrometer was effectively rebuilt to incorporate a wideband AWG. The lab was then locked down due to Covid and we have not since been in a position to remeasure. We have measured T_M in the same system as a function of offset at Q-band and as expected it shows T_M becoming very significantly shorter with offset in line with results originally reported by Raitsmiring. We also now report in the SI, Q-band measurements with both pump and probe at offset frequencies (on one side of the central resonance). We cannot rule out that the substantial gain in sensitivity observed at W-band compared to Q-band is partly due to a difference in relaxation rates. We would point out that the excellent S/N observed at W-band is despite the expected reduction in T_M.

We have made it clear that T_M was not measured at offset frequencies, and included a statement that we would expect T_M to be transition dependent for this model system along with relevant reference(s).

6. **section 205: For systems other than Gd(III), Tm also can rarely be fitted with a single exponential function. Please rephrase to avoid the impression that this is a peculiar feature of Gd(III).**

We agree this statement was not clear and we will rephrase.

7. Section 210: Why did you use fixed exponents 1 and 2 for fitting? I do not see a good theoretical reason for that. Fit quality is hard to ascertain in Fig. S2a (please use a representation as in Figure 3a, black versus red line), However, looking closely I am not convinced that it is good. Please check if the fit residual is reasonably close to white noise.

The fit is actually extremely good ($R^2 = 0.9999$). If we look at the residual, we see a tiny bit of ESEEM at the very start, and then (at very small amplitude but well above the noise) we see a modulation that corresponds to the electron dipolar coupling. The residual is close to white noise at the end of the trace after the dipolar oscillation has decayed.

If we fit to the sum of two exponentials with different exponents, and let the exponents be free parameters, we get best fits where the exponents are found to be extremely close to 2 and 1. There is work by Salikhov that suggests that when $Wt >> 1$ then the exponent is expected to be 1 and when $Wt << 1$ then you expect the exponent to be equal to 2 (where W is the rate of the dephasing process). We think it reasonable to suggest that the exponent 2 component is attributable to nuclear dipolar coupling and it is not unreasonable to believe there could be a very fast component. However, on reflection we agree that we should be more cautious in attributing a specific mechanism to this component.

The basis for our speculation is we previously found (in unpublished results) that this same double exponent fit also offers excellent fits for large multi-spin systems with nitroxide spin labels (independent of sample concentration, but where the fast fluctuation depends on excitation bandwidth) and also provides a much better fit than a single stretched exponential. But we haven't yet done similar experiments with Gd.

We have now used a similar representation as Fig 3a to make the data points clearer and have given statistical measures to indicate the fit is actually very good. We have also added comments indicating why exponents 1 and 2 were chosen.

8. **Figure 3a: The fits for P1O1 and P2O2 do not compare favorably to the one shown by Dalaloyan et al. for the same compound (DOI: 10.1039/c5cp02602d). Do you have any idea why that may be the case?**

We would actually claim that the experimental data and fit for 6 nm-ruler are almost identical to the equivalent experimental data and fit of Dalaloyan at W-band (allowing for differences in modulation depth and S/N). It maybe the referee, was actually looking at the experimental data and fit for measurements made at Q-band, given in the same paper, for the same system. This does give a different modulation and, visually, a better fit. It also gives a different distance to that found at W-band. Previous computational modelling in Manukovsky 2017, that took into account pseudosecular terms, had shown that small distortions are still expected even at 5 nm distances, under experimental conditions comparable to P101, P202 (and for the Q-band data shown in Dalaoyan). One thus might expect Q-band data to be more susceptible to pseudosecular effects as the central transition is broader, and that has been our experience for other measurements with Gd spin-labelled systems (not shown). So we are more confident about the W-band data.

9. **section 265: "We do not expect any orientation selection and so the Pake pattern spectra reported in Fig. 6a show strong distortions". This sentence is unclear. Please rephrase.**

We were trying to convey that the distortions observed are not expected to be due to orientation selection (as might be the case for nitroxides). But we completely agree the current phrasing is unclear and we have changed it.

10. **section 310: I recommend more cautious wording regarding the origin of the second component, as you do not have a comparison with a sample with only a single Gd(III).**

The current phrasing ("we speculate") was meant to convey a degree of caution, but as discussed above, we have changed the wording to indicate that more evidence is required.

11. Figure S3: How can you have a rising background for P3O3? This needs to be commented.

We had decided to include this background to be consistent with the methodology that was used in determining the background for all the other traces, together with a a comment in the caption stating this was unphysical. It is not completely clear why the background appears slightly different for this trace, compared to others. However, we agree that it casts unnecessary doubt on the results and we have now changed the fit to a slightly falling background.
We would stress this leads to almost exactly the same distance and distance distribution, but a slightly less perfect Pake pattern. We thus feel it does not change the underlying argument. The discrepancy probably arises because the time trace was not long enough to accurately determine the background as the oscillations have not completely died out.

We now just show a fit with a falling background with associated distance distribution and Pake pattern.

Reply to Comments from Stefan Stoll

This manuscript describes DEER distance measurements on rigid Gd-Gd rulers in a high-power W-band spectrometer with a weakly resonant probe. Excellent sensitivity is demonstrated. It is shown that short-distance artifacts due to dipolar state mixing are suppressed by using a large pump-observe separation and by avoiding the central transition.

The work is well executed. The manuscript is well written. It provides novel and important insights. I recommend publication, after the following comments are addressed.

We would like to thank Prof Stoll for his careful reading of the manuscript and many insightful comments, which we address below.

1. **Some of DEER experiments are performed outside the central transition, but Tm and T1 values are reported only for the central transition. What are Tm and T1 for the pump and observer positions on the non-central transitions?**

   We completely agree it would have been useful and appropriate to measure Tm away from the central transition at the offsets used. At the time of the experiments it was an oversight. Unfortunately immediately after these experiments the spectrometer was rebuilt to incorporate a wideband AWG and then the lab was locked down when COVID hit and so at the moment it is not possible to incorporate this data (at W-band). We have Q-band data and we will refer to this and other references. We would point out that T_M is expected to get shorter away from the central transition but we still achieve excellent S/N despite this.

2. **Line 111: Is it possible to give G/Wˆ1/2 conversion efficiencies for the shorted waveguide used in this work, and for a standard cylindrical cavity as reference?**

   It is possible to quote an effective conversion efficiency based on the typical length of the $\pi/2$ pulse (6 ns for a S=1/2 sample) in the waveguide, although of course the B_1 field varies significantly across the sample. For a fair comparison one should really quote this based on the power incident on the sample holder, which is not always clear when comparing systems, and of course it depends on the chosen bandwidth of the standard cavity. This type of comparison thus requires many caveats, which we are not keen to enter into in this paper. However, in the interests of discussion, a reasonable estimate in our system might be to assume 625 W at the sample, giving c ~ 0.6 $G/W^{1/2}$. This conversion efficiency is comparable to an X-band commercial cavity (optimised for concentration sensitivity) used in pulsed operation and with a comparable sample volume and comparable kW input power. As sensitivity scales with ω_0^2, very substantial sensitivity gains become possible as long as linewidth does not get very significantly broader. A critically coupled W-band cylindrical cavity might have a conversion efficiency that is 15 x larger than the waveguide sample-holder here (but with a much smaller sample volume and bandwidth).

   We have given a conservative estimate for c in the text.

3. **Line 272: How significant do the authors think are the differences between the data obtained at 840 MHz and 900 MHz offset? Are they within or outside the expected run-to-run scatter of the experiment?**

We think there are small differences, but we agree they are not large, and they were included partly as we had the data sets. The point of including measurements with seemingly similar offsets is that at 840 MHz and 900 MHz offset we are very close to the maximum bandwidth available from the EIK, where the power output starts to significantly degrade at band edges., so we are testing the bandwidth limits.

4. **Line 245: A pump-observe offset of 900 MHz is mentioned for the 6 nm ruler, but the data show 120 and 420 MHz offset only (Fig.3,4,S3a,S4).**

   Many thanks – we have corrected this typo.

5. **Figs.4 and 6: What do the shaded areas in a) and b) indicate?**

   It is essentially a guide to the eye, but we have added notes in the caption explaining

6. **Fig.5d and 7b: What does the black arrow indicate?**

The arrow indicates 94 GHz, the nominal centre frequency of our W-band EIK amplifier, which has a bandwidth of just less than 1 GHz. We have added an explanation in the captions to make this clear.

7. Fig.S3a: What is the reason the background in the P3O3 measurement is rising, as opposed to decaying?

The underlying reason is that the oscillations have not decayed fully by the end of the time trace and so it is difficult to determine accurately. We chose to show this background (with a note it was not physical) to be consistent about the way we determined backgrounds for all the other traces. i.e. by optimising the resulting Pake pattern.

We have now changed this to give a slightly decaying background. This now gives a marginally worse Pake pattern, but essentially exactly the same distance and distance distribution.

8. Table S3: What is T1 in the last column? Footnote 1 is not clear.

We agree and have changed the footnote.

9. Table S1: Separate last column into two, one with the linewidths, and with references.

We have done this.

10. Line 313ff: I don't quite understand the author's arguments concerning intra- molecular instantaneous diffusion contribution to dephasing. The modulation depth is only a few percent, so only a few percent of spins get excited by each pulse. Simultaneous excitation of both spins within the same molecule therefore has very low probability. Some clarification would be useful.

As per the discussion with Prof Jeschke we have attempted to be more cautious with this statement, but we would point out that we are measuring at the central transition and the presence of pseudosecular interactions shows that we cannot treat it as a simple dilute system.

11. **Line 391ff: What are "backshort positions", and what does it mean to "match out the echo signal"?**

In common microwave terminology a backshort is a short circuit termination in a waveguide whose position can be adjusted with respect to some reference plane. The reflection from the top of the sample and this termination can create a weak resonant circuit, which can significantly enhance the magnitude of the cross-polar signal. Thus sensitivity (echo signal) is thus maximised for certain positions of the backshort. We have added lines of explanation. In the text

12. **Line 397: Claiming that sub-µM concentrations are technically feasible is a bit overly speculative. That would correspond to a ca. 50-fold reduction in concentration compared to the presented data, and a 2500-fold extension of the measurement time, for example from 1 hour to 3 months. Doubling the repetition rate to 6 kHz (more is not feasible given the T1) shortens this to 1.5 months, still not feasible. I suggest removing the statement about sub-µM concentrations.**

The 1.5 month (or 3 month) time-scale suggested for a measurement at sub-µM concentrations would be correct if we needed to maintain the same S/N to extract useful information from the spectra. But the echo S/N after ~ 1.5 hours for 2.1 nm ruler is 8300. Even with only 2.1 % modulation, one would still have acceptable S/N if we reduced S/N by a factor of 10 reducing averaging time by a factor of 100, bringing averaging times < 1 day for sub-uM concentrations. Many published measurements are made with this averaging time. So we thus stand by our statement that sub-µM concentrations are feasible (right now).

To further emphasize this point we also now include additional comparative Q-band measurements in the SI. In one example, where both pump and probe are offset from the central transition, if we compare to our P3O data for 2.1 nm sample, we have a lower (echo) sensitivity by a factor of ~ 8 and a lower modulation depth by a factor of 3, leading to an effective reduction in S/N of 24. Satisfactory S/N was still obtained by averaging for approximately one day. We would suggest that S/N would still be acceptable with somewhat lower averaging times.

In the discussion, we also point out there are realistic ways to further improve sensitivity. Higher sensitivity would be expected with Gd-complexes with smaller zero-field splittings. There is scope to achieve higher sensitivity by using a wideband AWG to increase both pump and probe excitation bandwidths. Although not discussed in the paper, we also believe there is also scope to improve the conversion factor of the sample holders, whilst maintaining all their other advantages. We thus believe the sub-µM claim will ultimately prove to be relatively conservative.

We have added a sentence or two to make these points clearer, and have included Q-band data in the SI.

Reply to Comments from Alberto Collauto

The authors propose a very interesting application of a high-bandwidth, high-power W-band setup to measure undistorted Gd(III)-Gd(III) DEER traces even for short distances, condition under which the mixing of the (…) states caused by the pseudo-secular terms of the dipolar Hamiltonian results, under normal measuring conditions, in dampening of the dipolar modulation. A very interesting conclusion is proposed suggesting the use of the already available Gd(III)-based tags with low zero-field splitting even for short distances, provided that both the pump pulse and the detection sequence completely avoid the excitation of the central transition.

The manuscript is well written, and definitely suitable for publication on Magnetic Resonance; the conclusions are substantial and nicely supported by the presented data and analyses. However, there are some points that I would like to be addressed by the authors.

We thank Dr Collauto for his kind words above, and careful reading of the manuscript. We reply to his helpful and interesting comments below.

1. **The style of the references is not homogeneous: in some cases the full DOI hyperlink is reported, whereas in other ones only the DOI number is displayed; some references make use of journal abbreviations, whereas in other ones the full journal title is mentioned. Besides, the absence of spacing and/or indentation makes it really hard to find a specific item. Moreover, references having the same first author are not always listed chronologically. I advise to follow thoroughly the author guidelines.**

This appears to have been a problem with ENDNOTE. We believe we have now corrected any inconsistencies in the referencing.

2. **As far as I could see, no specific literature for Gd(III) labelling of DNAs has been cited although reference has been made in the text to this application (line 49).**

We have now added a reference.

3. **I found the nomenclature proposed in Table 1 rather unclear; for example, why is a 10 ns-long pump pulse set to the maximum of the central transition once identified as P1 and once identified as P3 (6.0 nm Gd ruler)? I would find easier for the reader to have the relevant experimental conditions reported for each experiment (pulse length and frequency offset) in the figure caption or as inset, and, to improve the readability of the manuscript, I would consider moving the sensitivity considerations reported in Table 1 to the supporting material.**

We have used such nomenclature P1 and P3 to emphasize that these two positions, although having similar pulse lengths, and positioned at the central transition, are at different frequencies. Note that the observer frequency is kept at 94 GHz and the pump frequency is varied so there are difference. We chose this naming scheme only after considering many alternatives.

With regard to the sensitivity, this is mentioned in the title and high concentration sensitivity is emphasized in the abstract, and we are not aware of any experimental results that show a higher concentration sensitivity for these systems. So we feel it is an important part of the

manuscript. These numbers allow other groups to directly compare sensitivity. The paper is not just about measuring short distances by having probe and pump away from the central transition. It is the fact that one can still make the measurement with very high sensitivity that we feel makes the result useful and interesting.

4. **Is the (rather lengthy) discussion about the echo decay traces relevant for the purpose of this paper? After all, the measurements were performed on the maximum of the central transition, whereas the DEER detection sequence was always placed at spectral positions where the largest contribution to the echo comes from other transitions. A possible solution could be to move this section to the supporting material.**

We would claim that relaxation times and thus discussion of echo decay traces is highly relevant to sensitivity with regards to the practicality and design of potential experiments made at low sample concentrations. We completely agree it would be better to give the relaxation times at offset frequencies. At the time this was an oversight. Unfortunately, immediately after the experiments the spectrometer was rebuilt to incorporate a wideband AWG and then we had the lab lock-down, and it has not been possible to make these measurements since.

5. **A high sensitivity of the experimental setup is claimed. However, a rather large sample amount (around 75 µL of a 40 µM solution, hence 3 nmol) was used compared to the typical ones used for conventional W-band or Q-band spectroscopy (around 5 µL of a 40 µM solution, hence 0.2 nmol; 15 times smaller!), or even X-band spectroscopy (around 20 µL of a 40 µM solution, hence 0.8 nmol). An extension of the proposed approach to applications where the limiting factor is the sample amount, such as investigations inside cells or on systems that are challenging to express and/or label, is therefore in my opinion still not straightforward.**

We can only agree that it would be nice to have both extremely high concentration sensitivity and very little sample. However, this comment does not appear to take into account the significant loss of concentration sensitivity for small volume cavities, especially at lower frequencies. If you are not sample limited then (with some caveats) maximising sample volume, at a given frequency, will always give a larger signal. We have now attached data in the SI where we show measurements taken at Q-band at high power (150 W), using Bruker's large volume Q-band cavity (with comparable sample volume to that used here – 50-60 µL). For 2.1 nm, with both pump and probe on one side of the central transition, the concentration sensitivity is reduced by around a factor of 72, compared, to the W-band measurement corresponding to P3O in the paper. One might expect the concentration sensitivity of the small volume Q-band resonator (quoted) to be down a further factor of 4. The concentration sensitivity of the X-band resonators quoted are likely to be very significantly worse. Of course, for systems that are difficult to express, having 50 uL sample volumes is not necessarily trivial – but as discussed in the paper there are potentially relatively straightforward ways to further improve sensitivity (and hence potentially reduce volume and improve absolute sensitivity) and still reach sub-µM sensitivity. So we believe this to be a very promising and flexible approach. That is not to say there aren't other promising approaches, like the W-band resonator approach taken by our collaborators at the Weizmann Institute. But we believe it will be very challenging to significantly improve the sensitivity at X-band and Q-band to make them competitive, both in terms of absolute and concentration sensitivity for these types of samples.

We have added some more lines in the discussion, discussing sensitivity.

6. **Throughout the main paper and the SI plots belonging to the same figure have different sizes and are not always aligned (see for example Figures 3 a/b, 5, S3, S4, S5).**

This has now been significantly improved.

Table 1: the shot repetition time should be given in time units; what is reported is the shot repetition rate.

Many thanks – we have corrected this typo and changed to shot repetition rate.

7. **Table 1: why was the shot repetition rate decreased from 3 kHz to 1 kHz for some of the measurements on the 2.1 nm Gd ruler (see Table 1)? Are measurements available to justify this choice?**

The simple answer is that the 1 kHz measurements could have been made with a repetition rate of 3 kHz (or an even higher rate as Stefan Stoll suggests) and we would have had the same signal to noise in less time. At the time we were being very conservative in our choice. That is one of the reasons we give sensitivity measures to allow different results to be compared. Results were not repeated, because immediately afterwards the experiments, the spectrometer front-end and detection system was rebuilt to incorporate a wideband AWG, which was a major change. We then had the COVID lab shut-down (and are still affected by it).

8. **Table 1: what was the used value of $\tau 1$ for the DEER experiments?**

The value is 300 ns and has been added to the figure caption.

9. **Were the DEER measurements performed with or without a phase cycling of the $\pi/2$ pulse? If without, which precautions were taken so as to have no constant offset of the DEER traces?**

We can measure with phase cycling, but these specific measurements were actually taken without phase cycling (for technical reasons). Instead, offsets were removed by separate automatic measurements of the baseline, on either side of the echo. This baseline was then subtracted (at the cost of a slight reduction in S/N). We would add that offsets are known to be very low, and signals were relatively high in these experiments and so the correction was rather small. We have added a line mentioning this.

10. **In Figure S3a the intermolecular contribution for the experimental condition P3O3 has been modelled as an increasing function, a clearly unphysical assumption (as also stated by the authors). The analysis of these experimental data has to be repeated by taking an exponential decaying function. Furthermore, the primary data are displayed only for t >= 0; is this the way in which the data were recorded? If so, why? If not, it would be advisable to plot the whole data, in such a way that the maxima of the recorded traces are visible.**

We chose to show the increasing intermolecular contribution (to be consistent with other results where contributions were chosen to give the best Pake pattern). However, we agree that this just casts an unnecessary question mark on that result. We have now fitted using a decaying contribution. This leads to a slightly less optimum Pake pattern, but effectively exactly the same distance and distance distribution. The underlying problem is of course that

the oscillations have not died out by the end of the trace, and so it is difficult to fit the background with absolute confidence. It is not clear why this trace has a slightly different background. However, we would point out that the intermolecular contributions in all these traces are much smaller than have been observed before in experiments on these samples and thus potential errors in estimating distributions are correspondingly much smaller.

We chose to only show $t > 0$, as the traces are very long and thus the period where $t < 0$ is correspondingly very short relative to the total trace, and correspond to only a few points, with little extra information content.

Nevertheless, we have now added these points.

12.Figures 5d and 7b: what do the black arrows highlight?

The arrows indicate 94 GHz which is the centre frequency of the EIK. This was added to be a guide to the eye, to show how the pump and probe pulses were positioned relative to the centre frequency. We have added a note in the captions.

13. Table S1: which distribution of E values was taken to fit the experimental data shown in Figure 2? Were the simulations perform assuming a monomodal distribution of D values around +D or a bimodal distribution of D values around ±D? (I am not able to deduce this information from lines 197-199 of the main text).

Whilst some previous studies on Gd-spin labels samples have needed a bimodal distribution centred on +D and –D to simulate the observed spectra, in this study, we found we could get an excellent fit by using a monomodal distribution around D. We have added a note to make it clear how the Gd spectra was modelled

14. Table S2: is the time corresponding to a decay of the echo signal to 10% of its initial value given as τ or 2τ? In which units is this value reported?

This parameter is a function of 2τ, and the units are μs. We have clarified this in the text.

15. Captions of the Tables S2/S3: what is x? Was the dead time 2τ 0 taken into account for the fit of the echo decay curves? (This is relevant as the traces were fitted with a non-exponential function).

The x parameter corresponds to time and it has now been changed to t to make this clear. The dead time was taken into account in the fits. (However, we didn't observe a major difference to the fits, both with and without the dead time).

16. Table S3: a bi-exponential behaviour of the inversion recovery curves has been reported. Were other kind of experiments attempted aimed at minimizing the role of spectral diffusion? Besides, a T1 value resulting from a mono-exponential fit of the experimental traces has been reported but no comparison between the biexponential and mono-exponential fits is shown in Figure S2.

At 40 uM concentration we do expect much (intermolecular) spectral diffusion, although we cannot completely rule it out. We have added a statistical measure for the mono-exponential to give a measure for the quality of the fit.

17. Figure S2: because of the poor resolution I can hardly see the experimental data points.

That is partly because the fit is so good (R^2=0.9999), but we have now changed the way the experimental data is presented to hopefully make this clearer.

18. Figure S2a: what was the minimum used value of τ? This can't be deduced from the figure, where the first point of the decay trace has been set at 2τ = 0.

The value of the interpulse τ was 300 ns and a note has been added to the figure caption.

19. Figure S2b: the inversion recovery curves have not been collected till a plateau corresponding to the full recovery of the echo signal has been observed. This may result in severe uncertainties in the estimation of the longitudinal relaxation rate by fitting of the experimental data (Table S3).

We agree that a slight error is possible, but the results are entirely consistent with Ref [Phys Chem Chem Phys, 18, 19037-19049] and were only used to estimate viable repetition rates. We have added a line of explanation.

20. Caption of Table S2 and lines 312-313 of the main text: why the fit of the echo decay curves has been described as a "sum of two stretched exponential functions" although for one of the components the exponent has been fixed to 1?

Many thanks. We agree the term "stretched" is confusing in this context and we have removed this.

21. Figure S3: given the amount of free space on the page, I would consider useful to quickly recap, maybe in the form of a table, the relevant settings corresponding to the different traces.

Tables have now been added in the available space showing the relevant settings corresponding to the different traces.

22. Figures S4, S5, S6: in my opinion, a reminder to the legend of Figure 2 for what concerns the color code used in the simulation of the EDFS-EPR spectra would be useful.

We have now added the legends, that were shown in Figure 2.

23. In my opinion, it would be useful to add the frequency response of the EIKA, which dominates the bandwidth of the system, to the plots in the supporting materials showing the excitation profiles of the pump and detection pulses. This would make immediately clear to the reader where the pulses have been positioned within the bandwidth of the transmission chain.

We have carefully considered this suggestion, but on balance we feel that this would make the resulting figures too cluttered. We have however pointed out in the caption that 94 GHz represents the centre frequency, and has been designated by a black arrow, where appropriate.

24. Figures 3, 5, 7, S4, S5, S6: how was the excitation profile of the detection sequence calculated?

An effective B_1 was calculated, derived from the length of the $\pi/2$ pulse that gave the largest signal, (allowing for the fact we are dealing with a high spin system). The predicted excitation profile for a refocussed echo was then calculated using simple spin mechanics, (Phys Chem Chem Phys., 2007, 1895-1910). The resulting excitation profile is narrower than the excitation profile of a simple π pulse or a simple Hahn spin echo, as expected.

We have added a line and the reference.

High sensitivity Gd^{3+}- Gd^{3+} EPR distance measurements that eliminate artefacts seen at short distances

Hassane EL Mkami[1], Robert I. Hunter[1], Paul A. S. Cruickshank[1], Michael J. Taylor[1], Janet E. Lovett[1], Akiva Feintuch[2], Mian Qi[3], Adelheid Godt[3], Graham M. Smith[1]

[1]SUPA, School of Physics and Astronomy, University of St Andrews, St Andrews KY16 9SS, UK.

[2]Department of Chemical Physics, Weizmann Institute of Science, Rehovot, Israel.
[3]Faculty of Chemistry and Center of Molecular Materials (CM_2), Bielefeld University, Universitätsstraße 25, 33615 Bielefeld, Germany.

Correspondence to: Hassane EL Mkami (hem2@st-andrews.co.uk) and Graham M. Smith (gms@st-andrews.ac.uk)

Abstract. Gadolinium complexes are attracting increasing attention as spin labels for EPR dipolar distance measurements in biomolecules and particularly for in-cell measurements. It has been shown that flip-flop transitions within the central transition of the high spin Gd^{3+} ion can introduce artefacts in dipolar distance measurements, particularly when measuring distances less than 3 nm. Previous work has shown some reduction of these artefacts through increasing the frequency separation between the two frequencies required for the Double Electron-Electron Resonance (DEER) experiment. Here we use a high power (1 kW), wideband, non-resonant, system operating at 94 GHz to evaluate DEER measurement protocols using two rigid Gd(III)-rulers, consisting of two bis-Gd^{3+}-PyMTA complexes, with separations of 2.1 nm and 6.0 nm, respectively. We show that by avoiding the $\left|-\frac{1}{2}\right\rangle \rightarrow \left|\frac{1}{2}\right\rangle$ central transition completely, and placing both the pump and the observer pulses on either side of the central transition, we can now observe apparently artefact-free spectra and narrow distance distributions, even for a Gd-Gd distance of 2.1 nm. Importantly we still maintain excellent signal-to-noise ratio and relatively high modulation depths. These results have implications for in-cell EPR measurements at naturally occurring biomolecule concentrations.

Keywords: Gadolinium (III), spin labels, ZFS, spin flip-flop, DEER

1 Introduction

DEER spectroscopy combined with Site Directed Spin Labelling (SDSL) is a powerful technique to probe structural and dynamic properties in a wide range of biological systems. Over the past decades, distance measurements have been mainly associated with nitroxide spin labels (SLs). This has led to the development of new experimental protocols and reliable data analysis programs for a routine extraction of distances and investigation of conformational changes. Amongst other reasons, the increasing interest in characterising proteins in their native environment has extended the spin labelling family to new labels based on paramagnetic metal ion complexes. Gd^{3+}-based SLs have been of particular interest as they already exist as a major class of contrast agents used in MRI and show a strong stability against the oxidation or reduction conditions found in cells, making them an ideal candidate for in-cell distance measurements.

Gadolinium is a half integer high spin S=7/2 metal ion, characterised by a broad distribution of zero-field-splitting (ZFS) parameters and an isotropic g value at high field (Raitsimring et al., 2005). At lower temperatures its EPR spectrum is dominated by the central transition $\left|-\frac{1}{2}\right\rangle \rightarrow \left|\frac{1}{2}\right\rangle$ superimposed on a broad featureless background coming from all the other transitions. To first order, perturbation theory shows the central transition is independent of the ZFS interaction, while the other transitions scale linearly with the axial ZFS parameter *D*. However, to second order the central line narrows as the operational frequency increases and its width scales proportionally with $\frac{D^2}{gB_0}$. Therefore, high frequencies have been favoured for distance measurements using Gd^{3+}-based spin labels due to an expected improved concentration sensitivity associated with placing the pump or observer frequency at the central line.

Since their introduction in 2007, several Gd^{3+}-based spin labels have been developed and a wide range of molecules have been successfully investigated, from simple model compounds to proteins, DNA, peptides and other biological systems (Gordon-Grossman et al., 2011;Potapov et al., 2010;Raitsimring et al., 2007;Yagi et al., 2011;Shah et al., 2019;Wojciechowski et al., 2015). The good agreement between distance distributions derived from Gd-Gd DEER data and those resulting from other techniques has motivated researchers to attempt investigation of in-cell proteins and peptides (Qi et al., 2014;Yang et al., 2019;Dalaloyan et al., 2019). In most of these studies, Gd^{3+} was treated like a S = 1/2 system and standard data analysis software packages, developed initially for nitroxides, have generally been applied. This approach has proven successful for Gd-Gd distances above 3-4 nm, but below 3-4 nm strongly damped dipolar distortions and artificially broadened distance distributions were obtained (Cohen et al., 2016;Dalaloyan et al., 2015;Feintuch et al., 2015;Manukovsky et al., 2017). This is caused by unwanted flip-flop transitions, whose effects are enhanced by strong dipolar coupling (Cohen et al., 2016;Manukovsky et al., 2017). This effect can be ameliorated by increasing the frequency offset between the pump and observer pulses (PO offset) (Cohen et al., 2016). This has usually been achieved by having the pump pulse positioned at the central transition and positioning the observer pulse with as large a frequency offset as possible. This is usually difficult to achieve with standard resonator bandwidths on commercial instruments. Nevertheless, a high frequency dual mode cavity with an ingenious design has been demonstrated, which can accommodate pump and observer pulses with separations of more than 1 GHz (Cohen et al., 2016). Unfortunately such cavities, particularly at high fields and low temperatures, can be challenging

to set up precisely. Relaxation-Induced Dipolar Modulation Enhancement (RIDME) is another experimental alternative where no such restrictions apply, since it is a single frequency technique, however it suffers from overtones of dipolar frequencies and requires a more complicated data analysis (Collauto et al., 2016;Keller et al., 2017;Meyer and Schiemann, 2016;Razzaghi et al., 2014).

In the present work, we demonstrate a simpler approach that uses a wideband non- or weakly-resonant sample-holder to show the benefit of wideband measurements. We use two Gd-rulers with calculated distances between two Gd(III)-PyMTA complexes of 2.1 nm and 6.0 nm (Qi et al., 2016;Dalaloyan et al., 2015). The Gd-Gd distances were calculated for a temperature at 160.4 K, the glass transition temperature of the mixture of glycerol-d8 and D_2O, 50/50 (v/v), applying the wormlike chain model as described previously (Dalaloyan et al., 2015). We explore two different experimental protocols. The standard approach where the pump pulse is positioned at the central transition, but with variable offset between pump and observer pulses of up to 900 MHz. In general, we observe narrower distance distributions and improved Pake patterns as frequency separation is increased. In the second approach we place the pump and observer pulses on either side of the $\left|-\frac{1}{2}\right\rangle \rightarrow \left|\frac{1}{2}\right\rangle$ central transition, avoiding excitation of the central transition altogether. In this case, we observe almost perfect Pake patterns, consistent with elimination of the artificial broadening of the distance distribution, even for the 2.1 nm Gd ruler. For this short 2.1 nm distance we show that any loss of sensitivity from not exciting the central transition is offset by the shorter time window now required to make the measurement.

2 Experimental

2.1 Sample preparation

The synthesis of the Gd-rulers has been described elsewhere (Qi et al., 2016). Solutions of 40 μM concentration (molecules) of the Gd-ruler (2.1 nm) and Gd-ruler (6.0 nm) were prepared in 50/50 (v/v) deuterated glycerol and D_2O (for chemical structure see Fig. 1). The use of the glycerol-d_8 /D_2O (1:1, v/v) was dictated by the desire to obtain a good glass, to reduce scattering losses, and to extend the phase memory time. For the Q-band measurements the samples were transferred to standard 3 mm quartz EPR tubes and flash frozen in liquid nitrogen prior to loading into the spectrometer. For the W-band experiments, the samples were transferred into 27 mm long fluorinated ethylene propylene (FEP) tubes with 3 mm outer diameter and 2 mm inner diameter and flash frozen in liquid nitrogen prior loading into sample-holder cartridges that were separately precooled in liquid nitrogen. These sample-holder cartridges were then loaded into the W-band spectrometer which had been pre-cooled to 150 K.

Formatted: Indent: First line: 1.27 cm

Formatted: Font: (Default) +Body (Times New Roman), 10 pt

Formatted: Font: (Default) +Body (Times New Roman), 10 pt

Formatted: Font: (Default) +Body (Times New Roman), 10 pt, Subscript

Formatted: Font: (Default) +Body (Times New Roman), 10 pt

Deleted: For the distance calculation, we applied the wormlike chain model, as reported previously in the Supplementary Information (SI) in …

Deleted: and computed the contour length of the Gd-rulers at the glass transition temperature of the mixture glycerol-d_8 and D_2O, 50/50 (v/v), i.e. 160.4 K as the expected distance for the Gd-rulers (Dalaloyan et al., 2015).

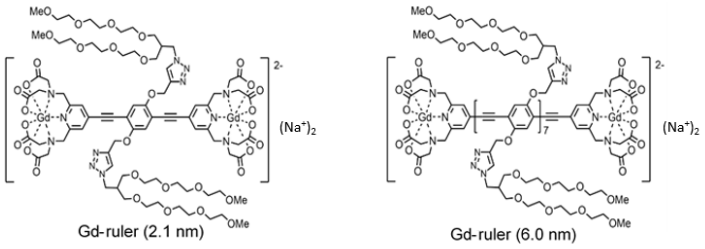

Figure 1: Chemical structures of Gd-ruler systems used in the current study.

2.2 Spectrometers

The spectrometers used for these measurements were a Bruker ELEXSYS E580 high power (150 W) Q-band pulsed spectrometer with ER 5106QT-2W resonator, and a home-built 1 kW W-band spectrometer (93.5 - 94.5 GHz). This W-band spectrometer, widely known as HiPER, has been described previously (Cruickshank et al., 2009;Motion et al., 2017). It operates with a wideband non-resonant (or weakly-resonant) induction mode sample holder, which is now described in more detail.

Deleted: (Cruickshank et al., 2009;Motion et al., 2017)

2.2.1 Non-resonant induction mode sample-holder

A non-resonant induction mode sample-holder is essentially a shorted symmetrical waveguide where two dominant orthogonal linearly polarised modes can propagate. The incident linearly polarised beam can be decomposed into two orthogonal circular polarisation components. At resonance, one circular component is absorbed (or emitted) by the sample, resulting in a reflected beam containing a cross-polarised component perpendicular to the linear polarisation of the incident beam. In the system described here these reflected signals are diplexed via a wire grid polariser to separate the high power incident beam from the very much smaller cross-polarised component which is passed to the detection system. The dimensions of the empty waveguide sample-holder (3 mm diameter) are chosen to be single-mode at the operating frequency of the spectrometer. The advantage of these shorted waveguide sample-holders are that they are inherently wideband since they are only weakly resonant. It might be thought that sensitivity would be strongly diminished as there is no resonant enhancement of either the excitation pulse or signal. However, the critical parameter that determines the resonant enhancement is the microwave conversion efficiency of the sample holder, c, with units $G/W^{1/2}$ (Smith et al., 2008). A single-mode shorted waveguide at 94 GHz can have a comparable or better conversion efficiency (5-6 ns $\pi/2$ pulse with 1 kW input) than a commercial X-band pulsed resonator. Compared to a dual-mode W-band resonator, a shorted waveguide can also offer a hugely increased sample volume (up to 75 μL in the current system), provided that sample dielectric losses are low, which is usually the case for measurements made at cryogenic temperatures. The non-resonant cavity also offers considerable flexibility in optimising excitation frequencies and bandwidths

at both pump and observer frequencies. Therefore these types of systems can have extremely high concentration sensitivity whilst offering very large instantaneous bandwidths. This potentially makes them ideal for Gd SL distance measurements, especially when large separations between the observer and pump pulses are required.

The sample is placed in a FEP tube within a sample-holder cartridge and mounted into a spring-loaded mount (see Fig. S1a). The latter co-locates to a smooth cylindrical waveguide transmission line of diameter 3 mm, which supports two orthogonal TE_{11} modes. Radiation is fed to the shorted waveguide via an adapted corrugated feedhorn that feeds to a wider bore corrugated pipe which in turn feeds to an optical system. An adjustable backshort consisting of a roof mirror with a shallow roof angle, is placed below the sample and its position can be adjusted vertically and rotationally by means of piezo-motors (Attocube Systems AG). The optimisation and isolation of the cross-polarised signal component are crucial both during the experimental set-up and measurements and this is mostly achieved by fine adjustment of the adjustable backshort using the Attocubes and of the quasi-optical components.

To facilitate the loading of pre-frozen samples, the samples and sample-holder cartridges are pre-cooled externally to the spectrometer in liquid nitrogen. The spring-loaded mount, feedhorn and corrugated pipe are housed inside a vacuum vessel which forms an extension to the sample flow cryostat and includes a vacuum window at the top to allow access for the microwave beams. The sample cryostat is cooled until the temperature of the spring-loaded mount reaches 150 K which has been found to be a reliable temperature to use for loading of pre-frozen samples. In order to load the sample the flow cryostat must be stopped and returned to ambient pressure using helium gas. The vacuum vessel is hoisted up along with the corrugated pipe, feedhorn and spring-loaded mount whilst a continuous flow of helium gas is maintained to minimise icing of the cryostat and microwave feed system. The sample-holder cartridge is removed from the liquid nitrogen and inserted into the spring-loaded mount along a guide channel where it becomes located into sockets, ensuring accurate alignment of the waveguide. The vacuum vessel is then lowered back down and sealed to the cryostat and is then evacuated. Cryogen flow is reinstated in the cryostat and the system is cooled to the measurement temperature.

2.2.2 Frequency dependent power variation in HiPER

It should be noted that the transmitted power level (from the amplifier / isolator / switch combination) is not constant over the whole range of the frequency offsets used in this study. This is illustrated in Fig. S1b where we show the power level versus frequency monitored at different points along the transmitter chain of HiPER. As a consequence of this, absolute modulation depths should not be compared quantitatively.

2.3 Pulse EPR experiments

For the Q-band experiments, echo detected field sweep (ED-FS) measurements were carried out at 10 K. The $\pi/2$ and π pulse lengths were set at 16 and 32 ns respectively, with an inter-pulse delay of $\tau = 200$ ns.

For the W-band experiments all measurements were performed at 10 K, which corresponds to the optimum temperature for these experiments when the central transition is excited (Feintuch et al., 2015;Goldfarb, 2014;Raitsimring et al., 2013). The

ED-FS spectra were recorded using a Hahn echo sequence with pulse lengths 6 and 12 ns as π/2 and π respectively and a delay of 300 ns. These pulse lengths were optimised by setting the magnetic field to the peak of the spectrum. The echo decay (T_m) and the inversion recovery (T_1) experiments were recorded at the central maximum of the ED-FS spectrum by stepping the associated sequences with steps of 100 ns and 1 µs respectively. It should be noted that differences are expected particularly for the phase relaxation when measuring away from the central transition (Raitsimring et al., 2014). The repetition rate for all W-band experiments was set at 3 kHz, unless otherwise stated, and this was again optimised at the maximum of the ED-FS spectrum.

Deleted: We have to notice

The DEER experiments were carried out using the standard dead-time free four-pulse sequence (Pannier et al., 2000).

Formatted: Indent: First line: 1.27 cm

$$\frac{\pi}{2}(obs) \rightarrow \tau_1 \rightarrow \pi(obs) \rightarrow t \rightarrow \pi(pump) \rightarrow \tau_1 + \tau_2 - t \rightarrow \pi(obs) \rightarrow \tau_2 \rightarrow echo$$

The echo intensity was monitored as a function of *t*. For the Gd-ruler (6.0 nm), the pump pulse was applied, for all experiments, at the maximum of the ED-FS spectrum whereas the observer frequency was set at 94 GHz with different offsets from the pump frequency as reported in **Table-1**. For the Gd-ruler (2.1 nm), different settings were investigated, with either the pump frequency being set at the maximum of the ED-FS spectrum and the observer frequency placed on the side of the central line, or with both the pump and observer frequencies being set on either side of the central line. The experimental parameters used in both cases are summarised in **Table-1**. Optimisation of the observer and pump pulse lengths was carried out systematically for each experiment given the wide range of frequency offsets used in this study. It is necessary to re-optimise the pulse lengths for each frequency offset, due to power variation from the transmitter chain. For technical reasons, these measurements were made without phase cycling, but instead offsets were removed by separate automatic measurements of the baseline on either side of the echo (at a slight cost in SNR).

DEER data were processed using the DeerAnalysis (2019) program that allows extraction of distance distributions (Jeschke et al., 2006). Fits to the data were based on standard Tikhonov regularisation analysis using the bending point in the L-curve. The excitation profiles of the pump and observer pulses were simulated using a home written MATLAB-based program using simple spin mechanics (Jeschke and Polyhach, 2007). The simulated ED-FS spectra and the associated sub-spectra for each transition were performed using the EasySpin program (Stoll and Schweiger, 2006).

Offset[1] (MHz)	Obs[2] π(ns)	Pump[3] π(ns)	τ_2(μs)	Data points	SRR[4] (kHz)	λ (%)	Echo SNR	Time averaging	Number of averages[5]	Sensitivity measure[6]
Pumping on the central line and observing on the side										
Gd-ruler (6.0 nm)										
120 (P_1O_1)	11	10	10.3	251	3	6.0	1111	1h30min (14 scans)	42000	2.06
120 (P_2O_2)	16	16	10.3	251	3	5.0	769	44min (7 scans)	21000	1.68
420 (P_3O_3)	11	10	10.3	251	3	4.5	2000	10h20min (99 scans)	297000	1.02
Gd-ruler (2.1 nm)										
120 (P_1O_1)	24	24	2.2	251	3	2.5	1923	1h (10 scans)	30000	1.75
420 (P_2O_2)	12	12	2.8	251	3	4.0	3125	1h (10 scans)	30000	4.56
840 (PO_5)	12	12	1.5	121	1	2.9	3279	1h40min (33 scans)	33000	4.68
900 (PO_6)	12	12	1.5	121	1	3.2	3846	0h45min (15 scans)	15000	8.99
Pumping and observing on the sides of the central line										
Gd-ruler (2.1 nm)										
800 (P_3O)	8	8	1.5	121	1	2.1	8333	1h26min (28 scans)	28000	9.35
900 (P_4O)	12	12	1.5	121	1	1.1	10000	4h27min (71 scans)	71000	3.69

Table-1: W-band experimental settings parameters used for DEER measurements on both rulers and the associated modulation depths obtained by fitting the DEER data with DeerAnalysis (Jeschke et al., 2006). The interpluse delay τ_1 was set to 300 ns for all experiments. To allow different DEER measurements to be compared more easily we take our sensitivity measure as the echo SNR multiplied by the modulation depth divided by the square root of the total number of measurements. It should be noted that this does not take into account differences in excitation bandwidth of pump and observer pulses.

[1] Frequency separation between pump pulse set at position i (P_i) and observer pulse at position j (O_j).

[2,3] Observer and pump π pulse lengths. The observer π/2 pulse was always half the observer π pulse.

Deleted: T

Deleted: Experimental

[4] SRR is the Shot Repetition Rate.

[5] Number of averages calculated as: number of scans * number of shots per point.

[6] The sensitivity measure is calculated as $=\frac{\lambda*SNR(Echo)}{(\sqrt{total\ number\ of\ points\ measured})}$ where SNR (echo) is the ratio of the maximum echo height to the standard deviation of the noise. This is obtained by subtracting a smoothed fit from the data and then calculating the standard deviation from the resulting noise trace. The total number of points measured is the total number of averages per point multiplied by the number of points in a scan.

3 Results

3.1 EPR spectra and relaxation times

The ED-FS spectra for both samples are similar to those reported for other Gd^{3+} complexes with a characteristic sharp line corresponding to the central transition and a broad featureless background resulting from contributions of all other transitions. The spectra recorded at Q- and W-bands are shown in Fig. 2. The simulation of the sub-spectra was performed using EasySpin by considering a distribution of the ZFS parameters D and E (Stoll and Schweiger, 2006). The magnitude and distribution of the ZFS depend primarily on the nature of the interactions between the Gd^{3+} ion and the ligand and / or solvent molecules coordinating to the Gd^{3+} ion. These are taken into account by the D and E strain parameters used by EasySpin and they are defined as monomodal Gaussian distributions. Furthermore, it was shown in some cases that a bimodal Gaussian distribution centred on D and $-D$ considerably improved the simulation (Raitsimring et al., 2005;Clayton et al., 2018). The D parameters used for the simulations are reported with those obtained for other Gd^{3+}-tags in **Table-S1**.

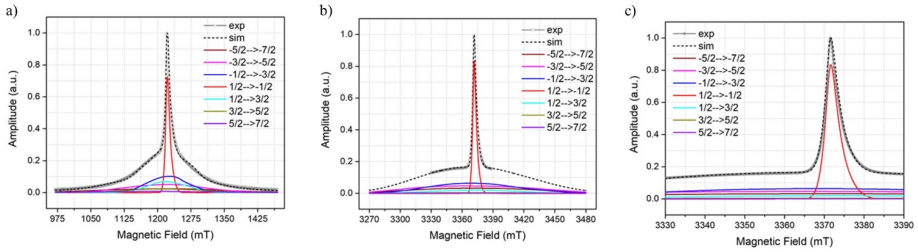

Figure 2: Simulated and experimental ED-FS spectra of the Gd-ruler (6.0 nm) with the associated sub-spectra of the individual transitions, a) at Q-band, b) at W-band with wide magnetic field ranges and c) at W-band with narrow magnetic field ranges respectively. The parameters used for the simulation are D = 1060 MHz, D_{Strain} = 850 MHz, E= 320 MHz and E_{Strain} = 200 MHz.

The phase memory time, T_m, and the spin lattice relaxation time, T_1, were measured for both samples at 10 K with the magnetic field set on the central maximum of the ED-FS and results were similar to other reported studies on Gd^{3+} complexes measured at low temperatures (Collauto et al., 2016;Raitsimring et al., 2014). The T_m time traces were fitted initially with a

Deleted: This
Deleted: Time
Deleted: , E =
Formatted: Subscript
Formatted: Highlight
Formatted: Subscript
Deleted: . In neither case was it possible to fit the data with a single exponential function. This finding, although it is not restricted to the Gadolinium, has also be
Deleted: en
Deleted: in other
Deleted: and seems to be typical commonly observed for
Deleted: therefore

sum of two exponential functions with free exponent values, and excellent fits were achieved with fixed exponent values of 1 and 2 and the results are shown in Fig. S2a. The fit to two exponentials ($R^2 = 0.9999$) was rather better than could be achieved by fitting to a stretched exponential. T_m values estimated from these fits are shown in **Table-S2**, and provide evidence for fast and slow relaxation contributions to the echo decay.

T_1 time traces were also well fitted to a bi-exponential function as shown in Fig. S2b. Fast and slow time constants were derived from these fits and are reported in **Table-S3**. It is emphasised that this relaxation data was taken at the central maximum, but T_m relaxation is expected to be faster away from the central maximum due to transition dependent fluctuations in the zero field splitting (Raitsimring et al., 2014).

3.2 Results from DEER spectroscopy

3.2.1 Gd-ruler (6.0 nm)

Background corrected DEER data obtained with Gd-ruler (6.0 nm) are shown in Fig. 3a and the corresponding primary data are shown in Fig. S3a. The pump and observer positions with their associated excitation profiles are reported in Fig. 3b, 3c and 3d. In addition to the excitation profiles, the pump and observer pulses positions, with respect to the central transitions $\left|-\frac{1}{2}\right\rangle \rightarrow \left|\frac{1}{2}\right\rangle$, are shown in Fig. S4. The modulation depths derived from the fits are summarised in **Table-1**. The data and fits at low frequency offsets are very similar, to those measured before at W-band, allowing for differences in SNR and modulation depth (Dalaloyan et al., 2015). The modulation depth λ of 6% obtained from the DEER data recorded with 120 MHz PO offset (see **Table-1**) is also in a good agreement with that derived from the concentration dependence of a similar parent Gd^{3+}-tag (Dalaloyan et al., 2015). By being slightly more selective with the pump pulse but keeping the same PO offset of 120 MHz, the modulation depth decreases to 5% as expected due to few spins being excited. When the PO offset is increased to 420 MHz the modulation depth drops to 4.5% mainly due to the output power drop off towards the band edges in our system. For this latter measurement, it should be noted the field was different than in the former two experiments, and the pump pulse is a different frequency (see Fig. 3b, 3c and 3d).

Deleted: stretched
Deleted: s
Deleted: however
Deleted: the best
Deleted: was
Deleted: , and
Deleted: indicate
Deleted: d
Formatted: Highlight
Deleted: with
Deleted: z
Deleted: T_M
Formatted: Font: Italic
Formatted: Font: Italic, Subscript
Deleted: (Raitsmiring,et al, 2014)
Deleted: (Dalaloyan et al., 2015)

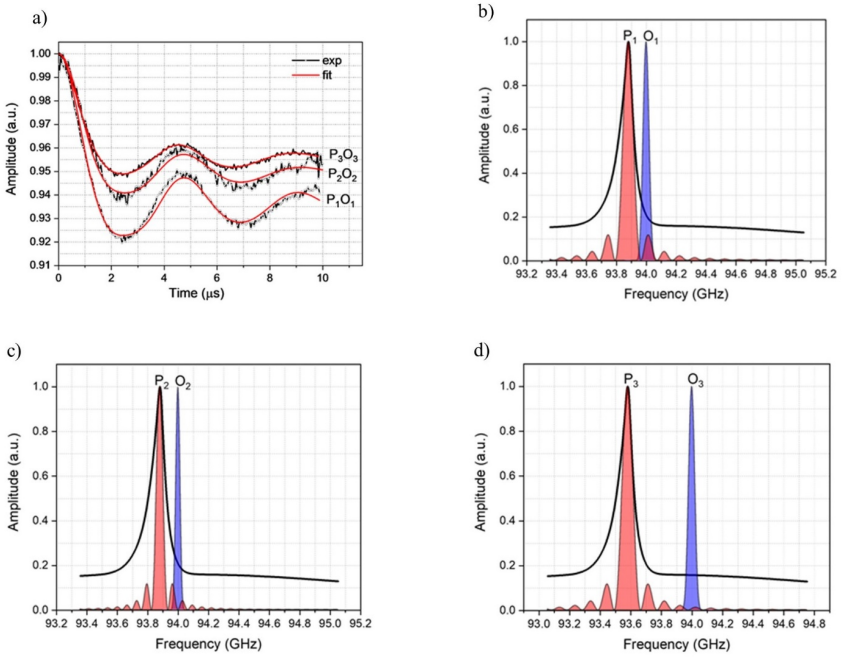

Figure 3: a) Background corrected DEER data (black curves) of Gd-ruler (6.0 nm) recorded with different PO offsets with the fits (red) obtained by DeerAnalysis (Jeschke et al., 2006). Excitation profiles of the pump (P) and observer (O) at different frequency offsets, b, c) P_1O_1 = P_2O_2 = 120 MHz with softer pulses for P_2O_2 and d) P_3O_3 = 420 MHz.

The derived Pake pattern spectra and the associated distance distributions are shown in Fig. 4**.** The distance distribution derived from DEER data measured with 120 MHz PO offset appears to be deviating slightly from 6.0 nm, the expected distance for this Gd-ruler, with a full width half height (FWHH) of 0.56 nm whereas with 420 MHz offset it is well centred on 6.0 nm with a FWHH of 0.48 nm. The Pake patterns, for all experimental settings, show normal and typical shapes with clear dipolar singularities corresponding to parallel and perpendicular orientations. These DEER measurements were recorded, as mentioned, with the pump position set at the peak of the FS-ED spectrum, which primarily excites the $\left|-\frac{1}{2}\right\rangle \rightarrow \left|\frac{1}{2}\right\rangle$ transition whereas the observer frequency for both offsets was positioned where the $\left|-\frac{3}{2}\right\rangle \rightarrow \left|-\frac{1}{2}\right\rangle$ transition contributes most

Deleted: b, c, d)

Formatted: Subscript

Formatted: Subscript

Deleted: Details of pump (P) and observer (O) pulses are summarised in Table 1.

Formatted: Subscript

Formatted: Subscript

Formatted: Subscript

Formatted: Subscript

Formatted: Subscript

Formatted: Subscript

to the detected signal (see Fig. S4a,b). The Gd^{3+} spectrum is the result of a superposition of several transitions with different weights, and their contributions, either to the pumped and observed spins, are expected to be magnetic field dependent. By increasing the PO offset, while keeping the pump position at the maximum of the FS-ED spectrum, the contribution of the $\left|-\frac{3}{2}\right\rangle \rightarrow \left|-\frac{1}{2}\right\rangle$ transition to the detected signal gradually decreases whilst the contributions of the other transitions, $\left|-\frac{7}{2}\right\rangle \rightarrow \left|-\frac{5}{2}\right\rangle$, $\left|-\frac{5}{2}\right\rangle \rightarrow \left|-\frac{3}{2}\right\rangle$, increase.

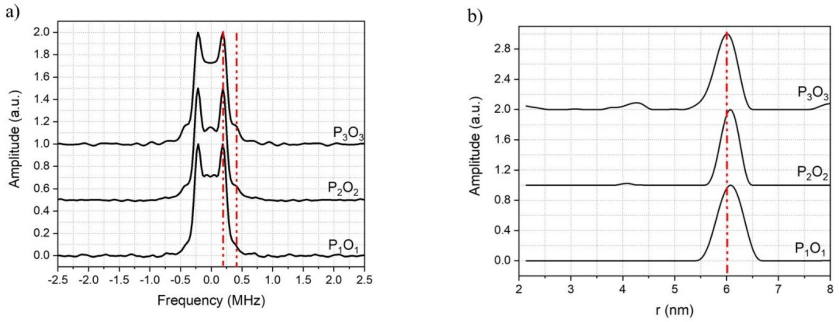

Figure 4: a) Pake pattern spectra obtained from fitting of the DEER data of the Gd-ruler (6.0 nm) sample measured with different offsets between pump and observer pulses and b) corresponding distance distributions derived from the DEER data. The PO offsets are $P_1O_1 = P_2O_2 = 120$ MHz and $P_3O_3 = 420$ MHz. The red vertical dashed lines show in a) the positions of the parallel and perpendicular singularities of the Pake pattern and in b) the expected distance.

3.2.2 Gd-ruler (2.1 nm)

The DEER measurements with Gd-ruler (2.1 nm) were conducted with a combination of different pump and observer positions and several PO offsets. Figure 5a shows background corrected DEER data obtained with measurements performed with the pump pulse set at the position of the central transition with PO offsets of 120, 420, 840 and 900 MHz. The corresponding primary DEER data are shown in Fig. S3b**.** The excitation profiles of the pump and the observer at these positions are reported in Fig. 5b, 5c and 5d. The pump and observer positions with respect to the central transition are shown in Fig. S5. At 120 MHz and 420 MHz PO offsets, the time domain DEER data show severely damped dipolar modulations (see Fig. 5a) whereas in the cases of 840 and 900 MHz offsets, the dipolar modulations are significantly recovered however they are still not as well defined as one might expect for a stiff model system. The obtained modulation depths λ are reported in **Table-1**.

Deleted: from 120 MHz up to 900 MHz

Deleted: P

Deleted: The positions of the pump (P) and observer (O) are shown in Fig. 2b, 2c and 2d.

Formatted: Subscript

Formatted: Subscript

Formatted: Subscript

Formatted: Subscript

Formatted: Subscript

Formatted: Subscript

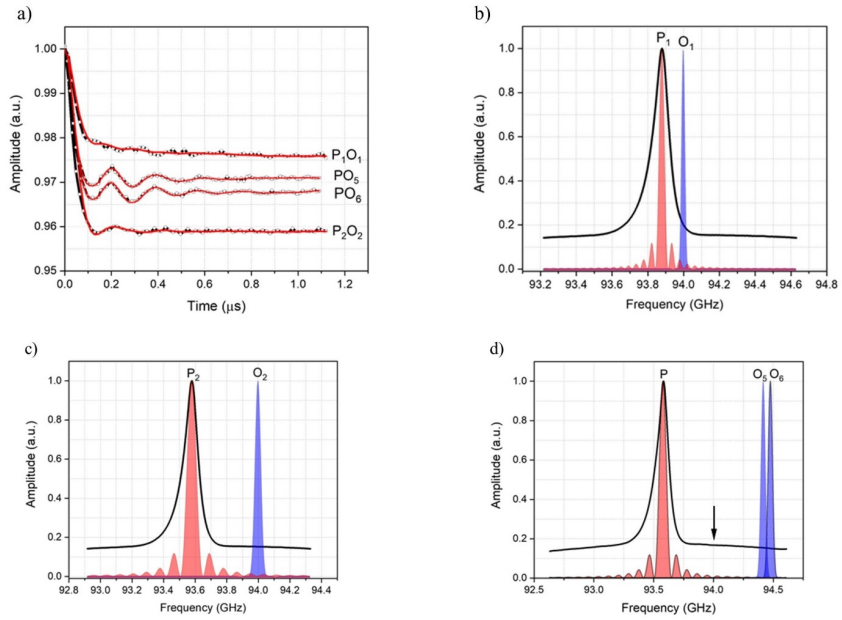

Figure 5: a) Background corrected DEER data (black curves) of Gd-ruler (2.1 nm) recorded with different offsets between pump and observer pulses together with fits (red curves) obtained by DeerAnalysis (Jeschke et al., 2006). b, c and d) Excitation profiles of the pump (P) and observer (O) pulses at different frequency offsets. Please note the different frequency scales. The corresponding frequency offsets are P_1O_1 = 120 MHz, P_2O_2 = 420 MHz, PO_5 = 840 MHz and PO_6 = 900 MHz. The black arrow indicates the position of 94 GHz, the nominal centre frequency of our W-band EIK amplifier, which has a bandwidth of just less than 1 GHz.

The Pake pattern spectra reported in Fig. 6a show strong distortions and poorly resolved dipolar singularity points for the 120 and 420 MHz PO offsets. In contrast we observe substantially improved Pake pattern spectra for the larger offsets of 840 and 900 MHz, particularly concerning the perpendicular dipolar singularities. In Fig. 6b, the distance distributions are considerably broadened for the 120 and 420 MHz PO offsets, with FWHH, determined only for the major peak centred at 2.1 nm, of 0.83 and 0.45 nm. However, at 840 MHz PO offset, the peak in the distance distribution is centred at the expected 2.1 nm distance with a FWHH of 0.24 nm. The best results were obtained with the 900 MHz PO offset giving a distance distribution

Deleted: Details of the pump (P) and observer (O) pulses are summarised in **Table-1**

Formatted: Subscript

Formatted: Subscript

Formatted: Subscript

Formatted: Subscript

Formatted: Subscript

Formatted: Subscript

Deleted: ¶

Deleted: We do not expect any orientation selection and so the

with a FWHH of only 0.17 nm. Note that results for 840 MHz and 900 MHz are given as this is close to the edge of the EIK amplifier bandwidth.

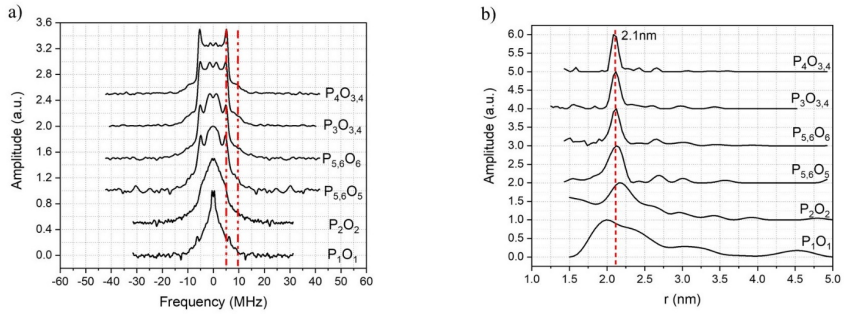

Figure 6: a) Pake pattern spectra obtained from the fitting of the DEER data of the Gd-ruler (2.1 nm) sample measured with different offsets between pump and observer pulses and b) associated distance distributions derived from the DEER data. The corresponding frequency offsets are P_4O_4 =120 MHz, P_2O_2 = 420 MHz, PO_5 = 840 MHz, PO_6 = 900 MHz, P_3O = 800 MHz and P_4O = 900 MHz. The red vertical dashed lines show in a) the positions of the parallel and perpendicular singularities of the Pake Pattern and in b) the expected distance.

A further set of DEER experiments were performed by setting the pump and observer pulses on either side of the central transition with large PO offsets. With this we aimed to exclude completely the contribution of the $\left|-\frac{1}{2}\right\rangle \rightarrow \left|\frac{1}{2}\right\rangle$ transition of both the pumped and observed spins (see Fig. S6). Figure 7a shows the DEER data corresponding to 800 and 900 MHz frequency PO offsets. The pulse profiles associated with the pump and observer pulses are presented in Fig. 7b. For both PO offsets the obtained dipolar modulations show more than four clear oscillations and smooth damping, highly reminiscent of spectra of structurally related nitroxide-rulers with similar distances (Godt et al., 2007).

Deleted: ,
Deleted:
Deleted: of the EIK amplifier.
Deleted: positions of the pump (P) and observer (O) pulses are shown in Fig. 4b, 4c and 4d.
Formatted: Subscript
Formatted: Subscript
Formatted: Subscript
Formatted: Subscript
Formatted: Subscript
Formatted: Subscript
Formatted: Subscript
Formatted: Subscript

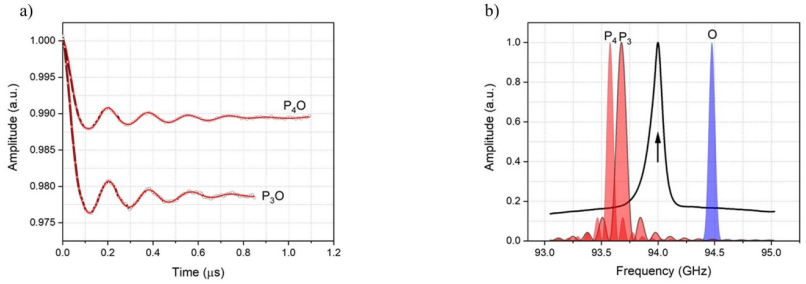

Figure 7: a) Background corrected DEER data (black curves) of Gd-ruler (2.1 nm) recorded with different offsets between pump and observer pulses together with fits (red curves) obtained by DeerAnalysis (Jeschke et al., 2006). b) Excitation profiles of the pump (P) and observer (O) pulses at different frequency offsets. The corresponding frequency offsets are P_3O = 800 MHz and P_4O = 900 MHz. The black arrow indicates the position of 94 GHz, the nominal centre frequency of our W-band EIK amplifier, which has a bandwidth of just less than 1 GHz.

The Pake patterns reported in Fig. 6a show the expected shape with well resolved perpendicular and parallel dipolar singularities. The corresponding distance distributions, shown in Fig. 6b, show a very narrow major peak centred at 2.1 nm with FWHH of 0.17 and 0.11 nm respectively. We also checked for signs of asymmetry in the distance distribution associated with flexibility of the ruler backbone, as previously found with nitroxide rulers (Godt et al., 2007). This asymmetry is not clearly evident with Gd-ruler (2.1 nm), possibly because the ruler is too short, as mentioned by one of the referees. However, there are signs of asymmetry for Gd-ruler (6.0 nm) in the measurement corresponding to P_3O_3 at large pump observer offsets. This asymmetry becomes less clear at smaller pump observer offsets as can be seen from Fig 4. This is further evidence that even at long distances it can be beneficial to have large offsets between pump and observer.

4 Discussion

High quality DEER spectra from 40 µM concentration samples were obtained with averaging times of an hour or two. Modulation depth, SNR of the echo and experimental parameters are given in **Table-1**. As different traces were measured with different numbers of scans and different shot repetition times, or have different number of points in the scan, we also provide a sensitivity measure for DEER measurements that normalises for these quantities. Results can be compared to W-band measurements on the same Gd system (Dalaloyan et al., 2015). The high concentration sensitivity, relative to conventional W-band resonator-based spectrometers is attributed to much larger effective sample volumes (~ 50 - 80 µL) and larger excitation bandwidths facilitated by the high available power that is only partially offset by the lower conversion factor. Large effective

Deleted: nm
Formatted: Subscript
Deleted: pump (P) and observer (O) pulses are summarised in **Table-1**….
Formatted: Subscript
Deleted: observed
Deleted: -
Deleted: (Godt et al., 2007)
Deleted: ,

volumes are possible with biological systems in non-resonant sample-holders at W-band, as dielectric losses are expected to be small at cryogenic temperatures ($\tan\delta < 0.001$) if a high quality glass is formed.

The echo decays (measured at the central transition), shown in Fig. S2a, were well fitted with a sum of two exponential functions with exponents found to be extremely close to 1 and 2 (R^2=0.9999). Little difference in phase memory time was observed between the two rulers, with a slightly lower decay for Gd-ruler (2.1 nm). However, no correlation had been found between the echo decay rate and the Gd-Gd distance of the same type of ruler as used in our study (Dalaloyan et al., 2015). This type of decay appears to be a characteristic of the Gd^{3+} complexes, and very similar results have been obtained before (Collauto et al., 2016;Raitsimring et al., 2014;Dalaloyan et al., 2015). Nuclear spin diffusion is often the dominant process in phase relaxation of the central transition (Garbuio et al., 2015), when one would expect the data to be well fitted with a single stretched exponential with an exponent of close to 2 (Kathirvelu et al., 2009). However nuclear spin diffusion is expected to be significantly reduced by matrix deuteration, and contributions resulting from thermally assisted fluctuations in the zero-field splitting are then expected to become significant (Raitsimring et al., 2014). The need to fit with two stretched exponentials suggests an additional fast dephasing process is contributing to the transverse relaxation. We tentatively speculate that this additional dephasing process is driven by intra-molecular instantaneous diffusion due to the electron spin flip-flop processes resulting from simultaneous excitation of $\left|-\frac{1}{2}\right\rangle \rightarrow \left|\frac{1}{2}\right\rangle$ transitions belonging to both Gd^{3+} ions of one Gd-ruler. This seems to be consistent with the T_m values derived from the fits (see **Table-S2**) which show identical slow parts for both samples as one would expect for the same matrix and different fast parts as a result of two Gd^{3+} systems with different dipolar couplings, due to different Gd-Gd distances, and therefore different spin flip-flop rates. The inter-molecular instantaneous diffusion process is less effective at concentrations as low as used in this study and is therefore considered to not contribute. However, this hypothesis needs further investigation at different concentrations, and on a similar sample with a single Gd^{3+} label.

Inversion recovery data shown in Fig. S2b have been well fitted with the sum of two mono-exponential functions with fast and slow components (see **Table-S1**). In addition, we provided a single T_1 value that was determined from a mono-exponential function fit to the inversion recovery data. It is interesting to note that the longer T_m component is comparable to the shorter T_1 component.

For DEER experiments, the weak coupling approximation is generally expected to hold when the PO offset between the coupled spins is significantly larger than the dipolar coupling between the coupled spins. This is usually fulfilled for Gd^{3+}-Gd^{3+} distance measurements where a frequency offset of at least 100 MHz is often used. In both Gd-rulers, Gd-ruler (2.1nm) and Gd-ruler (6.0 nm), the expected dipolar couplings are 5.6 and 0.2 MHz respectively and are far below the smallest frequency offset of 120 MHz used in our measurements. However, in the present work, as well as in the literature, artefacts in the spectra are observed for distances below 3-4 nm (Raitsimring et al., 2007;Dalaloyan et al., 2015;Cohen et al., 2016;Manukovsky et al., 2017). Such artefacts mainly manifest themselves as a damping of the dipolar modulations in the time domain, which in turn results in an artificial broadening of the distance distributions. This has previously been explained in terms of unwanted excitation of flip-flop transitions within the central line. For the highest sensitivity in Gd^{3+}-Gd^{3+} DEER

Deleted: best fit to the
Deleted: obtained
Deleted: stretched
Deleted: being fixed to
Formatted: Superscript
Deleted: e deviation from the mono-exponential
Deleted: T
Deleted: M

measurements, the pump pulse is usually set at the maximum of the ED-FS spectrum to ensure the deepest modulation depth (and the observer is often set just outside the central line). Under such conditions, the central transition, $\left|-\frac{1}{2}\right\rangle \rightarrow \left|\frac{1}{2}\right\rangle$, contributes most to the pumped spins, whereas, just away from the central transition, the $\left|-\frac{3}{2}\right\rangle \rightarrow \left|-\frac{1}{2}\right\rangle$ transition becomes the more dominant contribution to the observer spins (see Fig. S4a,b). The DEER signal is thus the result of the difference between the energy levels associated with the two transitions $\left|-\frac{3}{2}(A),\frac{1}{2}(B)\right\rangle \rightarrow \left|-\frac{1}{2}(A),\frac{1}{2}(B)\right\rangle$ and $\left|-\frac{3}{2}(A),-\frac{1}{2}(B)\right\rangle \rightarrow \left|-\frac{1}{2}(A),-\frac{1}{2}(B)\right\rangle$. The associated energies of these two states are degenerate to first order of the ZFS and only a fairly small splitting is induced by the second order ZFS contribution and this falls within the range of the dipolar couplings corresponding to short distances between Gd^{3+} ions. Therefore, the weak coupling approximation is no longer satisfied and the secular pseudo-terms describing the flip-flop effects cannot be ignored. This has been confirmed theoretically and investigation has shown that the artefacts are only significant for short distances, where the dipolar coupling is large, and when either the pump or observer pulse is set on the $\left|-\frac{3}{2}\right\rangle \rightarrow \left|-\frac{1}{2}\right\rangle$ transition adjacent to the $\left|-\frac{1}{2}\right\rangle \rightarrow \left|\frac{1}{2}\right\rangle$ or vice versa (Cohen et al., 2016;Manukovsky et al., 2017). However, when other transitions are selected by the observer pulse, it was shown that these artefacts are strongly reduced (Manukovsky et al., 2017). This was originally experimentally confirmed in experiments with a dual-mode cavity (Cohen et al., 2016), and is also clearly seen in the experiments described here. This is particularly demonstrated in Fig. 5 where the pump pulse is set on the $\left|-\frac{1}{2}\right\rangle \rightarrow \left|\frac{1}{2}\right\rangle$ transition and the observer pulse is moved progressively further away from the central transition, which gradually reduces the contribution of the adjacent $\left|-\frac{3}{2}\right\rangle \rightarrow \left|-\frac{1}{2}\right\rangle$ transition (see Figs. S5).

For the short Gd-ruler (2.1 nm) clearer modulations and narrower distance distributions are observed as the frequency offset is increased. Clearly visible modulations in the time domain are observed, at the largest PO offset of 900 MHz (see Fig. 5a), although simulations have indicated that some residual effects from the pseudo-secular term can be observed even at such PO offsets (Manukovsky et al., 2017). Interestingly, small artefacts are even observed for the longer Gd-ruler (6.0 nm) distance in Fig. 3 where better fits to the expected Pake pattern are obtained at the larger 420 MHz frequency offset and the related distance distribution has its peak at the expected 6.0 nm distance (see Fig. 4b).

We note that in all the DEER studies reported so far, the central $\left|-\frac{1}{2}\right\rangle \rightarrow \left|\frac{1}{2}\right\rangle$ transition has always been selected, either for the pump or the observer pulse. It had generally been assumed that there would be too big a sensitivity penalty to do otherwise, and the advantage of operating at high fields was mainly associated with narrowing the line and achieving a higher degree of excitation of the central transition. This led to the view that it is necessary to choose a Gd spin label with a large ZFS when measuring short distances to reduce the effect of unwanted flip flops (Dalaloyan et al., 2015).

In this present work, we also investigated the DEER set-up where the pump and observer pulses are placed on either side of the central transition, thus avoiding any excitation of the central transition completely (see Fig. S6a). These DEER experiments, P_30 and P_40, shown in Figure 7a, now show time domain data with clear oscillations smoothly damped to the

limit value (modulation depth), giving clear Pake patterns and narrow distance distributions that are strikingly similar to those obtained for structurally related nitroxide-rulers with comparable spin-spin distances (Godt et al., 2006). This is evidence that when the central transition does not play a role in the Gd^{3+}- Gd^{3+} DEER measurements, the mixing of states has no major effect, as they do not share energy levels with those involved in the pump and observer transitions.

The ability to measure shorter distances with Gd-based spin-labels accurately has implications for sensitivity. Gd-ruler (2.1 nm) would be expected to have at least 10 times higher echo SNR, compared to Gd-ruler (6.0 nm) just from the shorter time window required for the DEER measurement, based on relaxation measurements at the central transition. This increase in sensitivity is likely to be even larger for biological samples that are usually highly protonated, and thus have significantly shorter phase memory times. The relative loss of sensitivity is therefore much less when shorter time windows become feasible, as shown with Gd-ruler (2.1 nm) where an echo S/N of 8330, and modulation depth of 2.1% was obtained after only one hour and a half, even with a reduced 1 kHz SRR.

For observer measurements made away from the central transition the relative gain, at short distances, also becomes larger as relaxation times are expected to shorten due to transition dependent phase relaxation (Raitsimring et al., 2014). In the measurements presented here, this is partially offset by the increased bandwidth required, and the reduced power available from the EIK / isolator / switch combination at the band edges of the EIK amplifier. The available power as a function of frequency is shown in Fig. S1b. However, interestingly, and perhaps counter-intuitively, we see little degradation in SNR, when neither pump nor observer are placed at the central transition. Modulation depth, although reduced is still reasonable, and thus we still obtain excellent overall sensitivity under this condition.

We therefore predict that Gd systems with smaller ZFS than used here (see Table-S1) are to be preferred because not only is it easier to avoid the central transition, but we would also expect the amplitude of other transitions to increase (per unit bandwidth), which will further increase sensitivity. We would also predict that relaxation effects due to thermally assisted fluctuations in the ZFS will reduce (Raitsimring et al., 2014). This is the subject of further investigation.

It should be noted, when pumping away from the central transition, at 40 µM molecular concentration, the required background correction to DEER traces is small relative to the experimental modulation depth. Indeed, the requirement for background correction is almost eliminated at short distances, as can be seen from the raw traces provided in Fig. S3b. This is particularly important for Gd^{3+}- Gd^{3+} DEER measurements where modulation depths are low, as small errors in background correction can make a significant contribution to uncertainties in the calculated distance distribution. The results can be compared to the larger corrections required at slightly higher spin label concentrations when pumping on the central transition (Dalaloyan et al., 2015).

There is also scope to further improve sensitivity, at W-band, by increasing both the shot repetition rate and averaging times, and operating at lower temperatures if the central transition is not excited. Backshort positions in the sample holder, (see Fig. S1a) were also optimised for cross-polar isolation rather than matching out the echo signal, which can make a difference of a factor of 2 in sensitivity. Other groups have demonstrated a significant sensitivity benefit from the use of broadband chirped pulses in DEER measurements on Gd^{3+} systems (Bahrenberg et al., 2017;Doll et al., 2015). These

Deleted: approximately

Deleted: (Raitsmiring et al., 2014)

Deleted: only

Deleted: actually measure higher echo

Deleted: ¶
This is the subject of further investigation, but we predict that since the Gd-rulers investigated have a moderate ZFS (1060 MHz) (see **Table-S1**), the experimental results when avoiding the central transition suggests that Gd systems with lower ZFS are to be preferred because it is then easier to avoid the central transition. In this case we would also expect the amplitude of other transitions to increase (per unit bandwidth), and relaxation effects due to thermally assisted fluctuations in the ZFS to reduce (Raitsimring et al., 2014), which will further increase detection sensitivity.¶
At 40 µM molecular concentration,

Deleted: relatively

Deleted: ,

Deleted: ,

Deleted: and relative to the correction required at higher spin label concentrations (Dalaloyan et al., 2015). The

Deleted: We point out the importance of measuring short distances in terms of improved sensitivity, in the context of biological compounds, including in-cell measurements. Biological samples are usually highly protonated, which leads to significantly shorter phase memory times than for the model compounds used in this study. This leads to a severe loss of sensitivity if long time windows are then required. The relative loss of sensitivity is much less when shorter time windows become feasible, as shown in this work.¶
We also note from the obtained sensitivity there is considerable scope to make high quality measurements at much lower concentration levels. …

Deleted: for

Deleted: improvement

Deleted: , when

methodologies particularly lend themselves to high power, wideband spectrometers like HiPER and promise significant further gains. In contrast, we found both sensitivity and signal fidelity were significantly reduced at Q-band relative to W-band, for the case where both pump and probe are placed on one side of the central transition (due to cavity bandwidth limitations). Example data sets, measured using a high power (150 W) commercial Q-band spectrometer with comparable sample volumes, are shown in the SI in Figure S7 and Table S4 for Gd-ruler (2.1 nm). For the case where both pump and probe are offset, sensitivity was reduced by a factor of 24 relative to W-band, using our defined sensitivity measure.

The sensitivity achieved at W-band suggests that it will be feasible to obtain high quality spectra for Gd^{3+} DEER measurements at sub-μM concentrations, even allowing for the shorter relaxation times commonly observed with spin-labelled biological samples. We have also observed promising results with Gd^{3+} spin-labelled biological samples, which we will report in a future publication.

5 Conclusion

In the present work we have investigated two Gd-rulers, with Gd-Gd distances of 2.1 and 6.0 nm, using Gd^{3+} complexes with a moderate ZFS of 1060 MHz. We have performed a variety of Gd^{3+}-Gd^{3+} DEER measurements with different offsets between pump and observer pulses, using a non-resonant induction mode cavity. This is a flexible wideband measurement set-up with relatively easy sample handling, where excellent signal-to-noise is observed.

We have shown, in agreement with previous experimental results, that larger PO offsets significantly reduce the artefacts observed for Gd-Gd distances below 3-4 nm, but appear also to be of benefit in the case of larger distances, such as 6.0 nm.

More importantly we have shown significantly improved distance distributions at short distances by completely avoiding excitation of the central transition in the DEER experiment, $\left|-\frac{1}{2}\right\rangle \rightarrow \left|\frac{1}{2}\right\rangle$, and mostly selecting $\left|-\frac{7}{2}\right\rangle \rightarrow \left|-\frac{5}{2}\right\rangle$, $\left|-\frac{5}{2}\right\rangle \rightarrow \left|-\frac{3}{2}\right\rangle$ and $\left|-\frac{3}{2}\right\rangle \rightarrow \left|-\frac{1}{2}\right\rangle$ transitions. This still gives very high signal-to-noise (per unit measurement time) while obtaining much improved fitting to expected Pake patterns. This is a strong motivation to select and/or develop Gd-based SLs with as small a ZFS as possible, and measure using wideband spectrometers at moderately high magnetic fields, where the central transition narrows. The sensitivity is already high but we envisage considerable scope for improvement.

Author contributions

MQ and AG designed and synthesised the Gd-rulers. HEM, RIH, PASC and GMS designed and built HiPER. HEM, RIH, JEL, AF and GMS devised the experiments which were performed by HEM, RIH and MJT. HEM and GMS chiefly wrote the manuscript, with further input from all authors.

Competing interests

The authors declare that they have no conflict of interest.

Deleted: systems

Deleted: for

Deleted: Even allowing for the shorter relaxation times commonly observed with spin-labelled biological samples t

Deleted: se

Deleted: results

Deleted: is technically

Deleted: and we will also

Deleted: report on these

Deleted: as field increases

Acknowledgements

It is a pleasure to acknowledge both Dr Duncan Robertson (University of St Andrews) for many useful discussions on hardware, and Professor Daniella Goldfarb (Weizmann Institute of Science) for many useful discussions on Gd-based spin labels. HM, GMS, JEL, RIH, PASC, and MJT are part of StAnD, which is a major collaboration between EPR groups at St Andrews and Dundee Universities.

Financial support

We would like to acknowledge EPSRC (EP/R)13705/1) for current funding on the HiPER project, and the Wellcome Trust for a multi-user equipment grant (099149/Z/12/Z) for upgrades on the Q-band system. We thank the Royal Society for an International Exchanges Grant and The Weizmann-UK Joint Research Program for allowing bilateral travel and research between the University of St Andrews and the Weizmann Institute of Science. JEL thanks the Royal Society for a University Research Fellowship. MJT thanks EPSRC for a CM-CDT studentship (EP/LO15110/1).

References

Bahrenberg, T., Rosenski, Y., Carmieli, R., Zibzener, K., Qi, M., Frydman, V., Godt, A., Goldfarb, D., and Feintuch, A.: Improved sensitivity for W-band Gd(III)-Gd(III) and nitroxide-nitroxide DEER measurements with shaped pulses, J Magn Reson, 283, 1-13, https://doi.org/10.1016/j.jmr.2017.08.003, 2017.

Clayton, J. A., Keller, K., Qi, M., Wegner, J., Koch, V., Hintz, H., Godt, A., Han, S., Jeschke, G., Sherwin, M. S., and Yulikov, M.: Quantitative analysis of zero-field splitting parameter distributions in Gd(iii) complexes, Physical Chemistry Chemical Physics, 20, 10470-10492, https://doi.org/10.1039/C7CP08507A, 2018.

Cohen, M. R., Frydman, V., Milko, P., Iron, M. A., Abdelkader, E. H., Lee, M. D., Swarbrick, J. D., Raitsimring, A., Otting, G., Graham, B., Feintuch, A., and Goldfarb, D.: Overcoming artificial broadening in Gd(3+)-Gd(3+) distance distributions arising from dipolar pseudo-secular terms in DEER experiments, Phys Chem Chem Phys, 18, 12847-12859, https://doi.org/10.1039/c6cp00829a, 2016.

Collauto, A., Frydman, V., Lee, M. D., Abdelkader, E. H., Feintuch, A., Swarbrick, J. D., Graham, B., Otting, G., and Goldfarb, D.: RIDME distance measurements using Gd(iii) tags with a narrow central transition, Phys Chem Chem Phys, 18, 19037-19049, https://doi.org/10.1039/c6cp03299k, 2016.

Cruickshank, P. A., Bolton, D. R., Robertson, D. A., Hunter, R. I., Wylde, R. J., and Smith, G. M.: A kilowatt pulsed 94 GHz electron paramagnetic resonance spectrometer with high concentration sensitivity, high instantaneous bandwidth, and low dead time, Rev Sci Instrum, 80, 103102, https://doi.org/10.1063/1.3239402, 2009.

Dalaloyan, A., Qi, M., Ruthstein, S., Vega, S., Godt, A., Feintuch, A., and Goldfarb, D.: Gd(III)-Gd(III) EPR distance measurements--the range of accessible distances and the impact of zero field splitting, Phys Chem Chem Phys, 17, 18464-18476, https://doi.org/10.1039/c5cp02602d, 2015.

Dalaloyan, A., Martorana, A., Barak, Y., Gataulin, D., Reuveny, E., Howe, A., Elbaum, M., Albeck, S., Unger, T., Frydman, V., Abdelkader, E. H., Otting, G., and Goldfarb, D.: Tracking Conformational Changes in Calmodulin in vitro, in Cell Extract, and in Cells by Electron Paramagnetic Resonance Distance Measurements, Chemphyschem, 20, 1860-1868, https://doi.org/10.1002/cphc.201900341, 2019.

Doll, A., Qi, M., Wili, N., Pribitzer, S., Godt, A., and Jeschke, G.: Gd(III)–Gd(III) distance measurements with chirp pump pulses, Journal of Magnetic Resonance, 259, 153-162, https://doi.org/10.1016/j.jmr.2015.08.010, 2015.
Feintuch, A., Otting, G., and Goldfarb, D.: Gd(3)(+) Spin Labeling for Measuring Distances in Biomacromolecules: Why and How?, Methods Enzymol, 563, 415-457, https://doi.org/10.1016/bs.mie.2015.07.006, 2015.
Garbuio, L., Zimmermann, K., Häussinger, D., and Yulikov, M.: Gd(III) complexes for electron–electron dipolar spectroscopy: Effects of deuteration, pH and zero field splitting, Journal of Magnetic Resonance, 259, 163-173, https://doi.org/10.1016/j.jmr.2015.08.009, 2015.
Godt, A., Schulte, M., Zimmermann, H., and Jeschke, G.: How Flexible Are Poly(para-phenyleneethynylene)s?, Angewandte Chemie International Edition, 45, 7560-7564, https://doi.org/10.1002/anie.200602807, 2006.
Godt, A., Schulte, M., Zimmermann, H., and Jeschke, G.: How Flexible Are Poly(paraphenyleneethynylene)s?, ChemInform, 38, https://doi.org/10.1002/chin.200710080, 2007.
Goldfarb, D.: Gd3+ spin labeling for distance measurements by pulse EPR spectroscopy, Phys Chem Chem Phys, 16, 9685-9699, https://doi.org/10.1039/c3cp53822b, 2014.
Gordon-Grossman, M., Kaminker, I., Gofman, Y., Shai, Y., and Goldfarb, D.: W-Band pulse EPR distance measurements in peptides using Gd(3+)-dipicolinic acid derivatives as spin labels, Phys Chem Chem Phys, 13, 10771-10780, https://doi.org/10.1039/c1cp00011j, 2011.
Jeschke, G., Chechik, V., Ionita, P., Godt, A., Zimmermann, H., Banham, J., Timmel, C. R., Hilger, D., and Jung, H.: DeerAnalysis2006—a comprehensive software package for analyzing pulsed ELDOR data, Applied Magnetic Resonance, 30, 473-498, https://doi.org/10.1007/BF03166213, 2006.
Jeschke, G., and Polyhach, Y.: Distance measurements on spin-labelled biomacromolecules by pulsed electron paramagnetic resonance, Physical Chemistry Chemical Physics, 9, 1895-1910, https://doi.org/10.1039/B614920K, 2007.
Kathirvelu, V., Sato, H., Eaton, S. S., and Eaton, G. R.: Electron spin relaxation rates for semiquinones between 25 and 295K in glass-forming solvents, Journal of Magnetic Resonance, 198, 111-120, https://doi.org/10.1016/j.jmr.2009.01.026, 2009.
Keller, K., Mertens, V., Qi, M., Nalepa, A. I., Godt, A., Savitsky, A., Jeschke, G., and Yulikov, M.: Computing distance distributions from dipolar evolution data with overtones: RIDME spectroscopy with Gd(iii)-based spin labels, Physical chemistry chemical physics : PCCP, 19, 17856-17876, https://doi.org/10.1039/c7cp01524k, 2017.
Manukovsky, N., Feintuch, A., Kuprov, I., and Goldfarb, D.: Time domain simulation of Gd(3+)-Gd(3+) distance measurements by EPR, J Chem Phys, 147, 044201, https://doi.org/10.1063/1.4994084, 2017.
Meyer, A., and Schiemann, O.: PELDOR and RIDME Measurements on a High-Spin Manganese(II) Bisnitroxide Model Complex, The Journal of Physical Chemistry A, 120, 3463-3472, https://doi.org/10.1021/acs.jpca.6b00716, 2016.
Motion, C. L., Cassidy, S. L., Cruickshank, P. A. S., Hunter, R. I., Bolton, D. R., El Mkami, H., Van Doorslaer, S., Lovett, J. E., and Smith, G. M.: The use of composite pulses for improving DEER signal at 94GHz, Journal of Magnetic Resonance, 278, 122-133, https://doi.org/10.1016/j.jmr.2017.03.018, 2017.
Pannier, M., Veit, S., Godt, A., Jeschke, G., and Spiess, H. W.: Dead-Time Free Measurement of Dipole–Dipole Interactions between Electron Spins, Journal of Magnetic Resonance, 142, 331-340, https://doi.org/10.1006/jmre.1999.1944, 2000.
Potapov, A., Yagi, H., Huber, T., Jergic, S., Dixon, N. E., Otting, G., and Goldfarb, D.: Nanometer-scale distance measurements in proteins using Gd3+ spin labeling, J Am Chem Soc, 132, 9040-9048, https://doi.org/10.1021/ja1015662, 2010.

Qi, M., Groß, A., Jeschke, G., Godt, A., and Drescher, M.: Gd(III)-PyMTA Label Is Suitable for In-Cell EPR, Journal of the American Chemical Society, 136, 15366-15378, https://doi.org/10.1021/ja508274d, 2014.
Qi, M., Hülsmann, M., and Godt, A.: Spacers for Geometrically Well-Defined Water-Soluble Molecular Rulers and Their Application, The Journal of Organic Chemistry, 81, 2549-2571, https://doi.org/10.1021/acs.joc.6b00125, 2016.
Raitsimring, A., Astashkin, A. V., Enemark, J. H., Kaminker, I., Goldfarb, D., Walter, E. D., Song, Y., and Meade, T. J.: Optimization of pulsed DEER measurements for Gd-based labels: choice of operational frequencies, pulse durations and positions, and temperature, Appl Magn Reson, 44, 649-670, https://doi.org/10.1007/s00723-012-0434-6, 2013.
Raitsimring, A., Dalaloyan, A., Collauto, A., Feintuch, A., Meade, T., and Goldfarb, D.: Zero field splitting fluctuations induced phase relaxation of Gd3+ in frozen solutions at cryogenic temperatures, J Magn Reson, 248, 71-80, https://doi.org/10.1016/j.jmr.2014.09.012, 2014.
Raitsimring, A. M., Astashkin, A. V., Poluektov, O. G., and Caravan, P.: High-field pulsed EPR and ENDOR of Gd3+ complexes in glassy solutions, Applied Magnetic Resonance, 28, 281, https://doi.org/10.1007/BF03166762, 2005.
Raitsimring, A. M., Gunanathan, C., Potapov, A., Efremenko, I., Martin, J. M. L., Milstein, D., and Goldfarb, D.: Gd3+ Complexes as Potential Spin Labels for High Field Pulsed EPR Distance Measurements, Journal of the American Chemical Society, 129, 14138-14139, https://doi.org/10.1021/ja075544g, 2007.
Razzaghi, S., Qi, M., Nalepa, A. I., Godt, A., Jeschke, G., Savitsky, A., and Yulikov, M.: RIDME Spectroscopy with Gd(III) Centers, The Journal of Physical Chemistry Letters, 5, 3970-3975, https://doi.org/10.1021/jz502129t, 2014.
Shah, A., Roux, A., Starck, M., Mosely, J. A., Stevens, M., Norman, D. G., Hunter, R. I., El Mkami, H., Smith, G. M., Parker, D., and Lovett, J. E.: A Gadolinium Spin Label with Both a Narrow Central Transition and Short Tether for Use in Double Electron Electron Resonance Distance Measurements, Inorganic Chemistry, 58, 3015-3025, https://doi.org/10.1021/acs.inorgchem.8b02892, 2019.
Smith, G. M., Cruickshank, P. A. S., Bolton, D. R., and Robertson, D. A.: High-field pulse EPR instrumentation, in: Electron Paramagnetic Resonance: Volume 21, The Royal Society of Chemistry, 216-233, 2008.
Stoll, S., and Schweiger, A.: EasySpin, a comprehensive software package for spectral simulation and analysis in EPR, Journal of Magnetic Resonance, 178, 42-55, https://doi.org/10.1016/j.jmr.2005.08.013, 2006.
Wojciechowski, F., Groß, A., Holder, I. T., Knörr, L., Drescher, M., and Hartig, J. S.: Pulsed EPR spectroscopy distance measurements of DNA internally labelled with Gd3+-DOTA, Chemical Communications, 51, 13850-13853, https://doi.org/10.1039/C5CC04234H, 2015.
Yagi, H., Banerjee, D., Graham, B., Huber, T., Goldfarb, D., and Otting, G.: Gadolinium tagging for high-precision measurements of 6 nm distances in protein assemblies by EPR, J Am Chem Soc, 133, 10418-10421, https://doi.org/10.1021/ja204415w, 2011.
Yang, Y., Yang, F., Li, X. Y., Su, X. C., and Goldfarb, D.: In-Cell EPR Distance Measurements on Ubiquitin Labeled with a Rigid PyMTA-Gd(III) Tag, J Phys Chem B, 123, 1050-1059, https://doi.org/10.1021/acs.jpcb.8b11442, 2019.